*J. Fluid Mech.* (1990), *vol.* 221, *pp.* 1–22
*Printed in Great Britain*



# On the evolution of the turbulent spot in a laminar boundary layer with a favourable pressure gradient

By Y. KATZ,† A. SEIFERT AND I. WYGNANSKI
Department of Fluid Mechanics and Heat Transfer, Tel-Aviv University, Ramat Aviv, Israel

(Received 20 December 1988 and in revised form 15 February 1990)

The evolution of a turbulent spot in an accelerating laminar boundary-layer flow was investigated. The type of boundary layer chosen for this experiment resembles in every respect the flow in the vicinity of a stagnation point theoretically described by Falkner and Skan. The rate of growth of the spot was significantly inhibited by the favourable pressure gradient in all three directions. It became much shorter and narrower in comparison with a similar spot generated in a Blasius boundary layer at comparable distances from its origin and comparable Reynolds numbers. The celerities of its boundaries did not scale with the local free-stream velocity as they do in the absence of a pressure gradient. Dimensional analysis was used to identify and correlate the independent variables determining the size, the convection speed, and the relative rate of growth of this spot.

The familiar arrowhead shape of the spot gave way to a rounded triangular shape with the trailing interface being straight and perpendicular to the direction of streaming. The familiar Tollmien–Schlichting wave packet was not observed in this pressure gradient because the surrounding boundary layer was very stable at the $Re$ considered. Since the arrowhead shape of the spot is associated with the breakdown of the waves within the packet it cannot occur below the critical $Re$. The relative size of the 'calmed region' following the spot also diminished; however, one could only speculate as to the origin of this region.

## 1. Introduction

The transition process from laminar to turbulent flow has been investigated during the past fifty years, but the thrust of these investigations was directed towards the laminar boundary layer evolving on a flat plate in the absence of a pressure gradient. Possible ways to delay transition and thus reduce the skin-friction drag provide the practical justification for this type of research, and the simplest configuration in which such a study can be implemented is a flat plate.

Turbulent spots represent the end product of most paths to transition (Morkovin 1969). They often appear spontaneously, seemingly bypassing the gradual amplification of disturbances resulting from a variety of instability mechanisms of the laminar boundary layer. It was observed (Elder 1962) that a sufficiently strong disturbance may trigger a spot instantly at subcritical Reynolds numbers at which all small-amplitude disturbances clearly decay. Consequently spots are often observed downstream of protuberances which generate vorticity and therefore

† Present address: Department of Aerospace and Mechanical Engineering, University of Arizona, Tucson, AZ 85721, USA.

destabilize the flow locally. They are produced in the laboratory by pulsed, large-amplitude disturbances introduced into the boundary layer by mechanical, acoustical or electrical means (e.g. Schubauer & Klebanoff 1956; Elder 1962; Wygnanski, Sokolov & Friedmann 1976; Cantwell, Coles & Dimotakis 1978; Gad-el-Hak, Blackwelder & Riley 1981). Quite different types of turbulent spots were observed in a flow of a thin film of water on an inclined surface (Emmons 1951) and in a plane Poiseuille flow (Carlson, Widnall & Peeters 1982), suggesting that the general characteristics of the spots depend on the type of flow in which they are generated.

Wygnanski, Haritonidis & Kaplan (1979), while exploring the possible mechanisms responsible for the proliferation and growth of turbulent spots in a laminar boundary layer, observed a pair of wave packets trailing the turbulent spot. These packets were identified with Tollmien–Schlichting (T–S) waves which broke down at high Reynolds numbers and generated new turbulent spots, setting a chain reaction by which turbulence contaminated the rest of the laminar flow. The intricate interplay between the single spot and its trailing wave packets was partially resolved by Glezer, Katz & Wygnanski (1989), who observed that the waves can break down, accelerate, and rejoin the turbulent spot provided that the critical Reynolds number (i.e. the $Re$ below which all T–S waves decay) of the laminar flow was exceeded. Below the critical Reynolds number, the waves are merely passive attendants to the spot (see Chambers & Thomas 1983) because they decay as they lag behind the unstable region (the 'moving generator' in the parlance of Glezer *et al.*) which accompanies the tip of the spot.

The significance of a pressure gradient in determining the critical Reynolds number is well known (Wazzan, Okamura & Smith 1968) but its effect on the size, shape and internal structure of the turbulent spot is not. An experiment was prepared at Tel-Aviv University with the cooperation of Dr Amini (see Wygnanski 1981) to investigate the turbulent structure of the spot in a favourable pressure gradient. It was believed that the accelerating boundary layer would slow the evolution of the spot and facilitate the mapping of its internal structures, hoping that some salient characteristics of these structures also exist in the absence of pressure gradient but in a more obscure fashion. A favourable pressure gradient was set up in the wind tunnel by placing a 3.6 m long flat plate at an angle of incidence of about 4° to the flow. The boundary layer generated at that time did not follow the self-similarity requirements imposed by the Falkner–Skan solution, even though the shape of the velocity profile resembled the theoretical Falkner–Skan profile for $\beta = 0.12$. Preliminary observations of the spot evolving in this boundary layer suggested that it grew at approximately one half the rate observed in a Blasius boundary layer at a comparable Reynolds number. Furthermore, the propagation velocity of the turbulent interfaces did not scale with the local free-stream velocity of the flow. Narasimha & Subramanian (1984) observed that the lateral growth of the spot decreased as a result of a favourable pressure gradient, which they imposed on their flow by inserting liners into the test section of their wind tunnel. Although the favourable pressure gradient used in that experiment did not generate a self-similar boundary layer the observed lateral spreading rates of the spot were consistent with the observations of Wygnanski (1981). Turbulent spots in plane Poiseuille flow were observed by Carlson *et al.* (1982) and were analysed in detail by Henningson (1988). These spots however, are quite different from the spots evolving in a boundary layer and consequently a direct comparison is all but impossible. The purpose of the present investigation was to establish the general relationships between the pressure

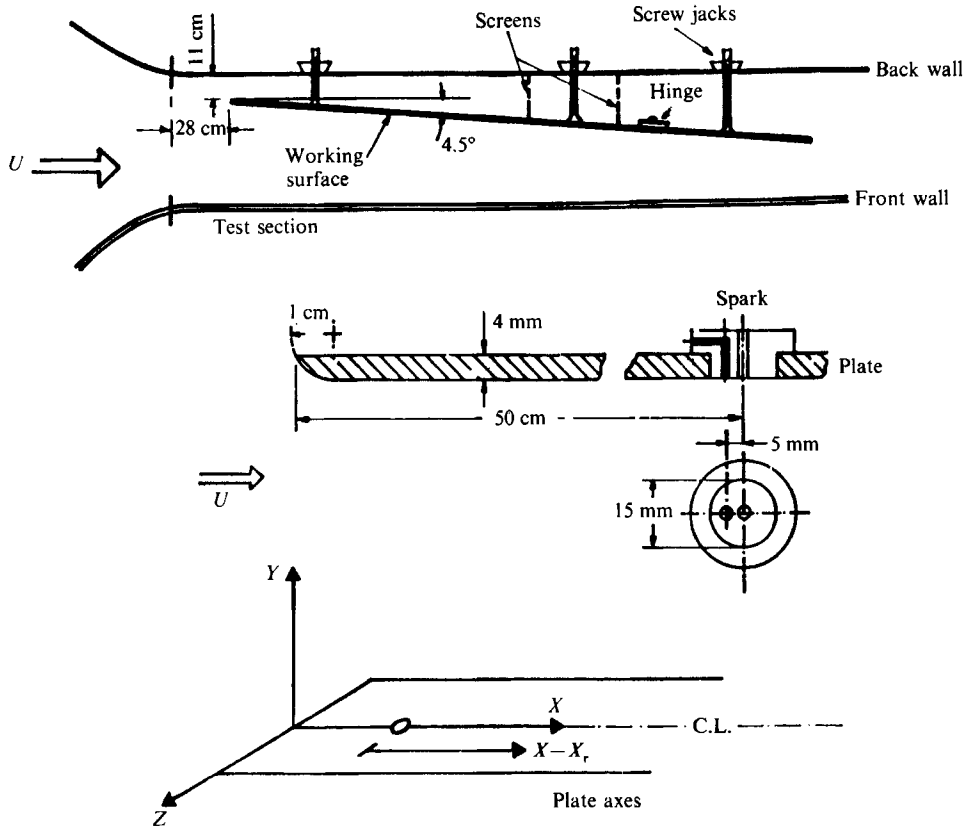


FIGURE 1. Description of the experimental apparatus.

gradient and Reynolds number on one hand, and the parameters characterizing the spot on the other. Some of these relationships will be discussed in the present manuscript.

The facility used in the present experiment was described by Wygnanski *et al.* (1976) and some of the novel data-reduction procedures were defined by Glezer *et al.* (1989) A polished aluminium plate was mounted vertically in the test section (figure 1). The plate could pivot around its leading edge, which was located 28 cm downstream of the inlet and 11 cm from the rear sidewall of the test section. The trailing edge of the plate was suspended from a curved track having a radius of curvature that is equivalent to the entire length of the plate. The angle of attack of the plate could therefore be easily changed within the constrained space limited by the sidewalls of the test section. An adjustable, trailing-edge flap was added in order to ensure that the location of the leading stagnation line occurs on the working surface but it was not used in the present experiment. Three sets of screw jacks mounted to the backward surface of the plate secured the plate to the sidewalls after the angle of attack of the plate was determined. Screens were added to the divergent channel between the backward surface of the plate and the rear sidewall of the test section in order to prevent flow separation from either surface and provide a pressure drop in that channel. The top and bottom walls of the test section are also adjustable and were used to regulate the pressure gradient until the measured thickness of the boundary layer did not vary in the direction of streaming. The gap between the plate

and the top and bottom walls of the tunnel had to be sealed after each adjustment in order to eliminate cross-flow between the two channels created in the test section by the presence of the plate. The time required to attain the desired pressure gradient was not prohibitive, in spite of the fact that the adjustment procedure was partially based on trial and error. The plate was inclined to the sidewalls of the test section at 4.5°.

## 2. Discussion of results

### 2.1. *The base flow*

The evolution of small disturbances in a laminar boundary layer depends on the detailed shape of the velocity profile, the thickness of the layer and the free-stream velocity. By invoking the parallel flow approximation the Orr–Sommerfeld equation is derived in which the mean velocity $U$ is normalized by the local free-stream velocity $U_1$, the derivatives with respect to the distance from the surface are normalized by the displacement thickness of the boundary layer $\delta^*$, and all times are scaled by $\delta^*/U_1$. The Reynolds number appears as a parameter in the equation. The validity of the solution was tested experimentally in the Blasius boundary layer (Schubauer & Skramstad 1947; Ross *et al.* 1970; Kachanov *et al.* 1975) and a correction had to be introduced to account for the divergence of the flow (Saric & Nayfeh 1975). A good generic flow against which the linear stability model could be tested is represented by the Falkner–Skan solution for the stagnation region (i.e. the Falkner–Skan parameter $\beta = 1$). However, this type of flow was never set up experimentally over a sufficiently long distance in the direction of streaming to provide the needed base flow for such a comparison. Furthermore, the required Reynolds numbers for such an experiment are an order of magnitude higher than for the Blasius boundary layer since the critical $Re_{\delta^*}$ increases from 520 at $\beta = 0$ to 13000 at $\beta = 1$. Nevertheless, if one is interested in exploring the reaction of the laminar boundary layer to strong disturbances, the steady-state solution for $\beta = 1$ is advantageous by being very stable to small-amplitude disturbances and by being parallel to the solid surface. The evolution of a turbulent spot in such a flow will not be clouded by the slow divergence of the base flow and by the possible secondary breakdown of Tollmien–Schlichting waves. The generation of such a flow will be discussed in this section.

The favourable pressure gradient was set up by inclining the plate with respect to the sidewalls of the wind tunnel, adjusting the divergence of the top and bottom walls, and adding screens behind the plate until the displacement thickness of the boundary layer $\delta^*$ did not vary with $X$. The ensuing normalized velocity profile

$$\frac{u}{U_1} = F'\left(\frac{kY}{\delta^*}\right) \tag{2.1}$$

turned out to be independent of $X$ and was therefore self-similar (figure 2).

The dependence of $U_1$ on $X$ can be easily derived by assuming the existence of a self-similar stream function: $\psi = U_r \delta^* [G(\xi) F(\eta)]$, (2.2)

where $U_r$ is a constant reference velocity defined at an arbitrary location outside the boundary layer; $\xi = (X - X_0)/\delta^*$ is a dimensionless distance in the direction of streaming and $X_0$ is the distance of the virtual origin from the leading edge of the plate; $\eta = kY/\delta^*$ is the similarity variable representing a dimensionless distance normal to the surface, and $k$ is a constant.

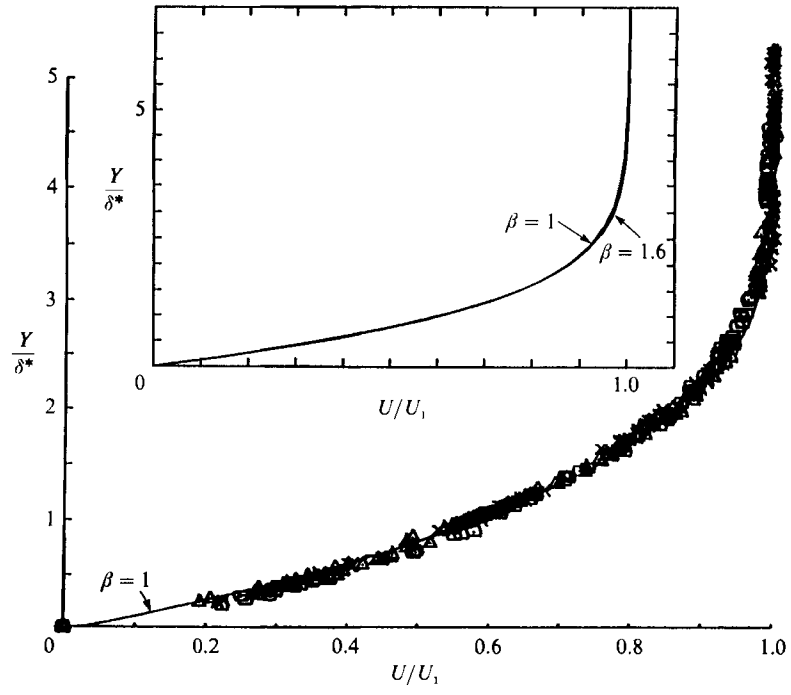


FIGURE 2. The dimensionless velocity profile measured between 100 and 200 cm from the leading edge of the plate at three reference velocities and compared with Falkner–Skan profiles having $\beta = 1$ and $\beta = 1.6$.

Substituting $\psi$ into the boundary-layer equations and requiring $\delta^*$ to be independent of $X$, results in the familiar Falkner–Skan equation describing the flow near a stagnation point provided:

$$\frac{dG}{d\xi} = \frac{k\nu}{U_r \delta^*} = \frac{k}{Re_{\delta^*}}$$

and

$$k \equiv \int_0^\infty [1 - F'(\eta)]\, d\eta, \tag{2.3}$$

where $F'(0) = 0$ ad $F'(\infty) = 1$. Consequently, the free-stream velocity gradient outside the boundary layer is

$$\frac{dU_1}{dX} = U_r \frac{k}{\delta^*} \frac{dG}{d\xi} = \nu \left[\frac{k}{\delta^*}\right]^2$$

or the dimensionless group

$$\left(\frac{\delta^{*2}}{\nu} \frac{dU_1}{dX}\right)^{\frac{1}{2}} = k. \tag{2.4}$$

The constant $k$, therefore, can be established experimentally from two independent quantities, first from the shape of the normalized, self-similar velocity profile and second from the constancy of the product $[(\delta^{*2}/\nu)(dU_1/dX)]$ which also implies that the free-stream velocity varies linearly with $X$, i.e.

$$U_1 = \frac{k^2 \nu}{(\delta^*)^2} (X - X_0), \tag{2.5}$$

where $X_0$ represents the location of the virtual origin of the flow.

One may normalize the data by choosing a location say, 100 cm from the leading edge as the characteristic location $X_{100}$ to obtain

$$\frac{U_1}{U_{100}} = \frac{X - X_0}{X_{100} - X_0}, \tag{2.6}$$

thus permitting the collapse of the data onto a single straight line as shown in figure 3(*b*).

The linear variation of $U_1$ along the plate was established experimentally for three free-stream velocities monitored at $X_{100}$ (figure 3). This location was chosen because it corresponds to the centre of the region in which the mapping of the turbulent spot was planned. The straight lines fitting the raw data are listed below:

$$U_{100} = 9.0\,\text{m/s}, \quad U_1 = 1.70(X + 4.24)\,\text{m/s}, \quad \delta^* = 1.6\,\text{mm}, \quad k = 0.544,$$

$$U_{100} = 7.5\,\text{m/s}, \quad U_1 = 1.47(X + 4.08)\,\text{m/s}, \quad \delta^* = 1.7\,\text{mm}, \quad k = 0.538,$$

$$U_{100} = 6.0\,\text{m/s}, \quad U_1 = 1.20(X + 4.00)\,\text{m/s}, \quad \delta^* = 1.9\,\text{mm}, \quad k = 0.543,$$

where $X$ is measured in m, and $k$ is determined from (2.4) using $\nu = 14.7\,\text{mm}^2/\text{s}$.

Thus, the virtual origin of the flow is located between $-4.24 < X_0 < -4.00$ m (i.e. upstream of the leading edge of the plate). Variations in the reference velocity affected the rate of change of the free-stream velocity with $X$ (i.e. $\mathrm{d}U_1/\mathrm{d}X$) and to a lesser extent affected the location of the virtual origin. Nevertheless, the value of $k$ remained unchanged, proving the validity of (2.4).

The theoretical value of $k$ derived from (2.3) for $\beta = 1$ should have been 0.6479 rather than the experimentally deduced value of 0.54. The discrepancy between the two estimates of $k$ is attributed to the lack of similarity near the leading edge of the plate where the stagnation streamline is forced to attach to the working surface. In this region the displacement thickness increases gradually before attaining its equilibrium value, while the free-stream velocity accelerates. These effects are manifested by the location of the virtual origin which is far upstream of the leading edge. The magnitude of $\delta^*$ reflects the upstream history of the flow and therefore affects directly the value of $k$ calculated from (2.4). The magnitude of $k$ derived from (2.3) is independent of the magnitude of $\delta^*$ by virtue of the definition of $\psi$.

Since the normalized shape of the velocity profile was self-similar at all reference velocities (figure 2) one may consider the *inverse problem* and attempt to determine the value of $\beta$ corresponding to $k = 0.54$, which turned out to be 1.6. Solving the Falkner–Skan equations for $\beta = 1$ and $\beta = 1.6$ yields two normalized velocity profiles which are experimentally indistinguishable (see the insert in figure 2). However, the evolution of the boundary layer in the direction of streaming would have been very different. For example, the free-stream velocity corresponding to $\beta = 1.6$ would have had to vary as the fourth power of $X$, while the boundary-layer thickness would have been proportional to $X^{-1.5}$, and this is certainly not the case in the present experiment. It is well known that the normalized shape of the Falkner–Skan family of velocity profiles is not sensitive to $\beta$ for $\beta > 1$, and fortunately small changes in $\beta$ around $\beta = 1$ do not affect the sensitivity of the calculated profiles to small perturbations (Wazzan *et al.* 1968). This is contrary to observations made in the absence of a pressure gradient (i.e. for $\beta = 0$), where the critical Reynolds number is very sensitive to small differences in $\beta$ which can be generated by imperceptibly small pressure gradients (Glezer *et al.* 1989). Consequently, the agreement between laminar

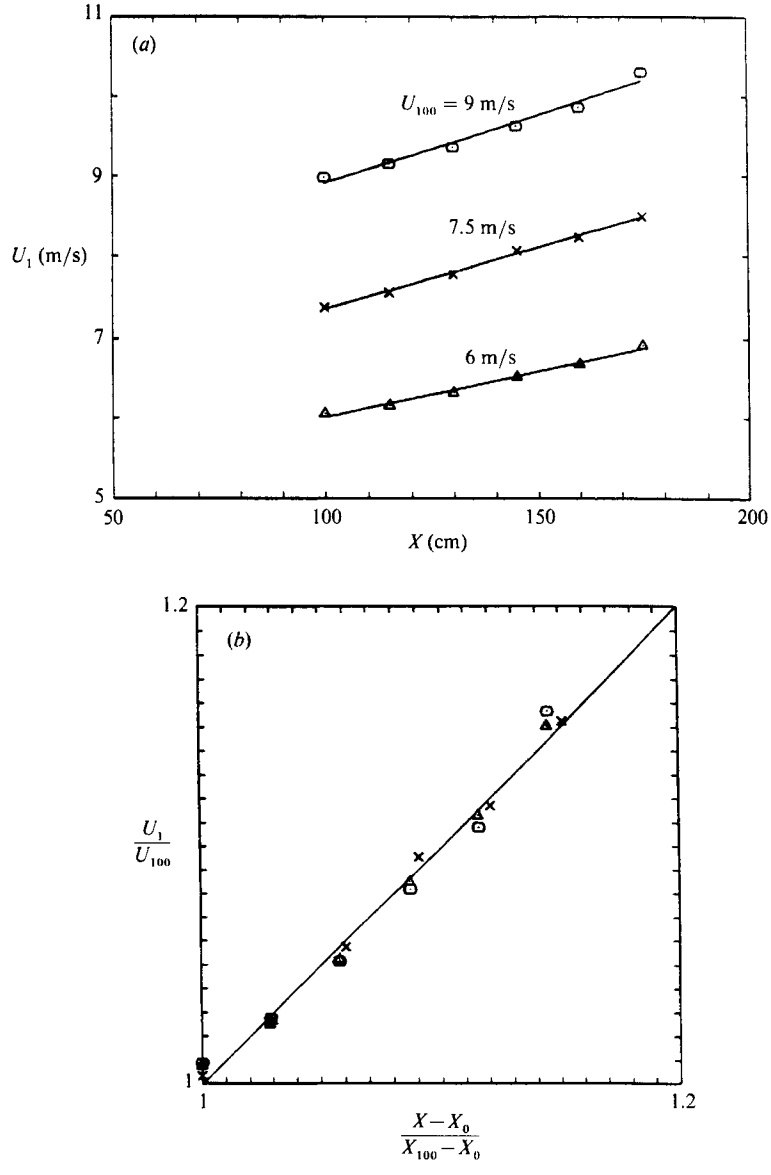


FIGURE 3. Variation of (*a*) free-stream velocity with $X$ and with the reference velocity and (*b*) dimensionless free-stream velocity with dimensionless distance.

boundary-layer theory and experiment is considered to be sufficiently good to assume that the turbulent spots observed in this experiment evolve as if they have occurred in a stagnation-point flow (figure 2).

The particular flow investigated experimentally is but one in a class of self-similar wedge flows which are characterized by a pressure gradient parameter $\beta$ such that

$$U_1 \propto [X-X_0]^{\beta/(2-\beta)}, \quad \delta^* \propto [X-X_0]^{(1-\beta)/(2-\beta)}, \tag{2.7}$$

which degenerate to (2.5) when $\beta = 1$. It is customary, in linear stability theory, to replace $X$ with $\delta^*$ as being an independent lengthscale governing the flow; the same

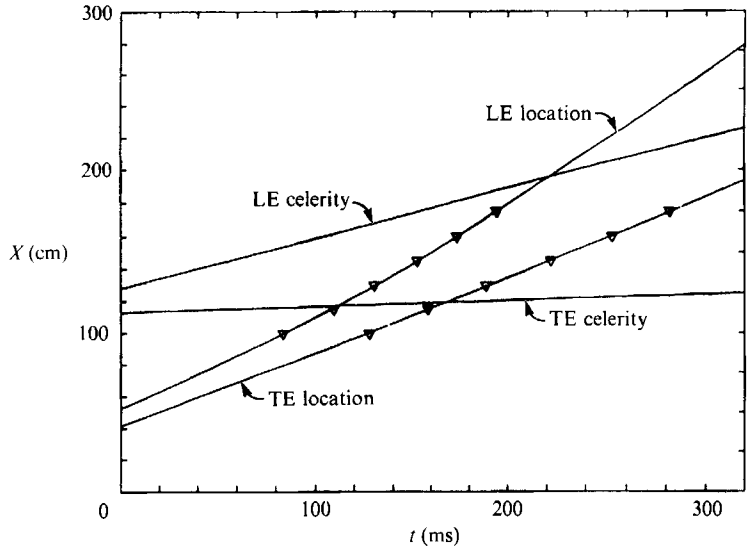


FIGURE 4. Determining the duration of the spot at a given $X$ or the length of the spot at a given time.

procedure will be followed in the present investigation. The most convenient reference velocity in this experiment corresponds to the free-stream velocity above the electrodes between which the turbulent spots are generated. This location in the past as the origin of the coordinate system used in studying turbulent spots. It will be used here for the sake of consistency, but any other choice of reference location for determining the free-stream velocity is equally valid.

### 2.2. *The effect of a pressure gradient on the size and shape of the spot*

The general shape of the spot, its rate of growth, and the celerity of its boundaries are reasonably well documented in the absence of a pressure gradient, but very little is known about the effect of pressure gradient on these spot characteristics. One can only surmise, from the pace at which the laminar boundary layer is contaminated by turbulence, that the rate of growth of the spot will be inhibited by a favourable pressure gradient and will be enhanced by an adverse pressure gradient.

The arrival time of the spot at a particular location and its duration at that location were determined by intermittency, which corresponds to an ensemble-averaged 'on–off' ('telegraph') signal defined by Glezer *et al.* (1989). Thus, for a probe situated at a given coordinate, two time instants are recorded, the first marking the arrival of the leading interface of the spot $t_{\mathrm{LE}}$ and the second marking the arrival of the trailing interface of the spot $t_{\mathrm{TE}}$. For example, the data plotted in figure 4 represent measurements taken at various $X$-locations on the plane of symmetry of the spot (i.e. at $Z = 0$) at constant $Y/\delta^*$ and $U_{100} = 7.5$ m/s. The average duration of the spot at a given location can be calculated directly by setting:

$$\Delta t = t_{\mathrm{TE}} - t_{\mathrm{LE}}, \tag{2.8}$$

while the average length of the spot at a given $(Y, Z)$-coordinate and time $t$ can be obtained by interpolation or by a polynomial fit to the data

$$(L_X)_{Y,Z,t} = X_{\mathrm{LE}} - X_{\mathrm{TE}}. \tag{2.9}$$

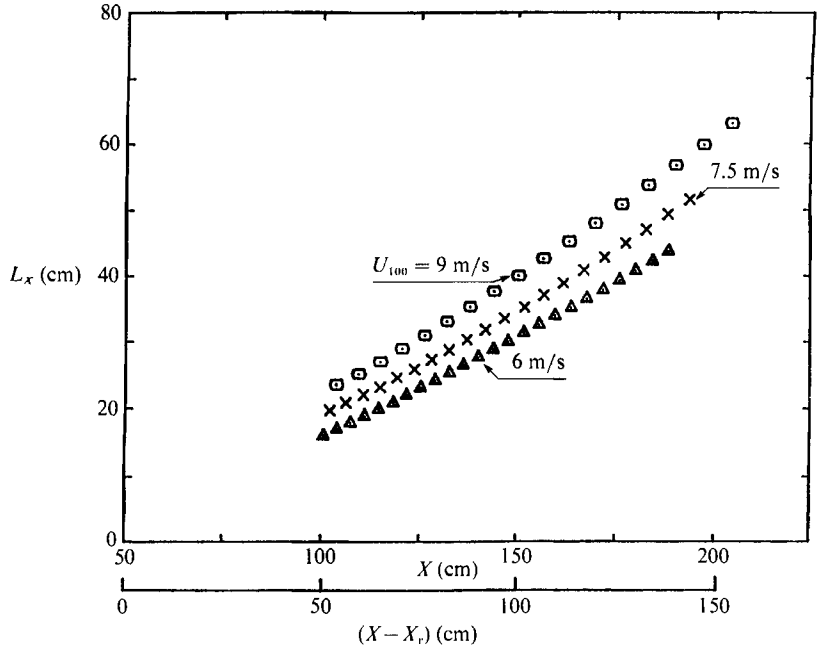


FIGURE 5. The length of the spot as a function of the distance from its origin.

$L_X$ may be expressed in a dimensionless form by dividing throughout by the distance of the spark (i.e. the location at which the spot was initiated) from virtual origin of the flow $(X_r - x_0)$:

$$\frac{L_X}{X_r - X_0} = \frac{X_{LE} - X_{TE}}{X_r - X_0}. \tag{2.10}$$

The time used for reference represents the interval between the initiation of the spot and the arrival of its most forward-reaching tip on the plane of symmetry (i.e. the 'overhang') to a prescribed $X$-location. This time is arbitrarily, though uniquely, defined as an independent variable. Experimental results on the plane of symmetry at $Y \approx \delta^*$ indicate that the spot becomes longer with increasing $X$ but the rate of its elongation is not constant, as is the case in the absence of the pressure gradient (figure 5). Furthermore, the local length of the spot depends on the free-stream velocity, in spite of the fact that the pressure gradient parameter $\beta$ is constant. An approximate rate of elongation of the spot in this experiment is described by $dL_X/dX \approx 0.35$, which is roughly equivalent to one-half of the rate observed in the absence of pressure gradient at comparable Reynolds numbers.

Furthermore, the celerities of the leading and the trailing interface may be determined from the slope of the curves shown in figure 4. These celerities can be expressed as functions of time or as functions of the location of the overhang. The shape and size of the spot at various stages of its development can be determined from such data by repeating the procedure mentioned above throughout the entire flow field.

The duration of the spot on the plane of symmetry at a given $U_r$ increases almost linearly with $X$, regardless of the elevation above the surface at which it was measured (the data shown in figure 6 provide information between $Y/\delta^* = 0.5$ and $Y/\delta^* = 8.5$). The longest duration of the spot at a given distance from the generator

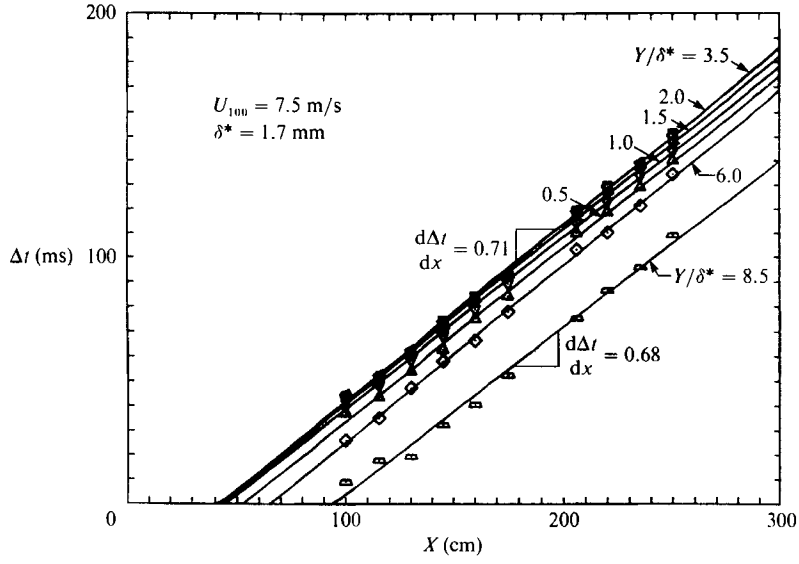


FIGURE 6. The duration of the spot at a given coordinate on the plane of symmetry ($Z = 0$). $U_{100} = 7.5$ m/s, $\delta^* = 1.7$ mm.

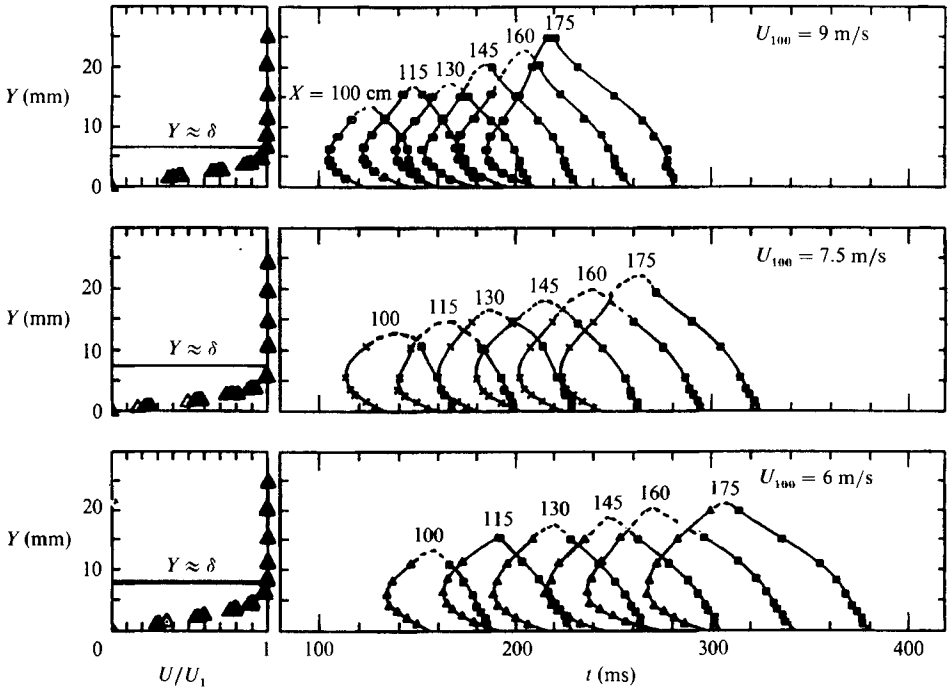


FIGURE 7. The temporal evolution of the spot in the $(t, Y)$-plane at $Z = 0$.

occurs at $Y/\delta^* = 3.5$, which concomitantly coincides with the edge of the laminar boundary layer and with the location of the 'overhang' from the surface. The temporal evolutions of the spots for the three reference velocities considered at all elevations from the surface are cross-plotted in figure 7. These results depict the growth of the spot with $t$ and $X$ showing its general shape on the plane of

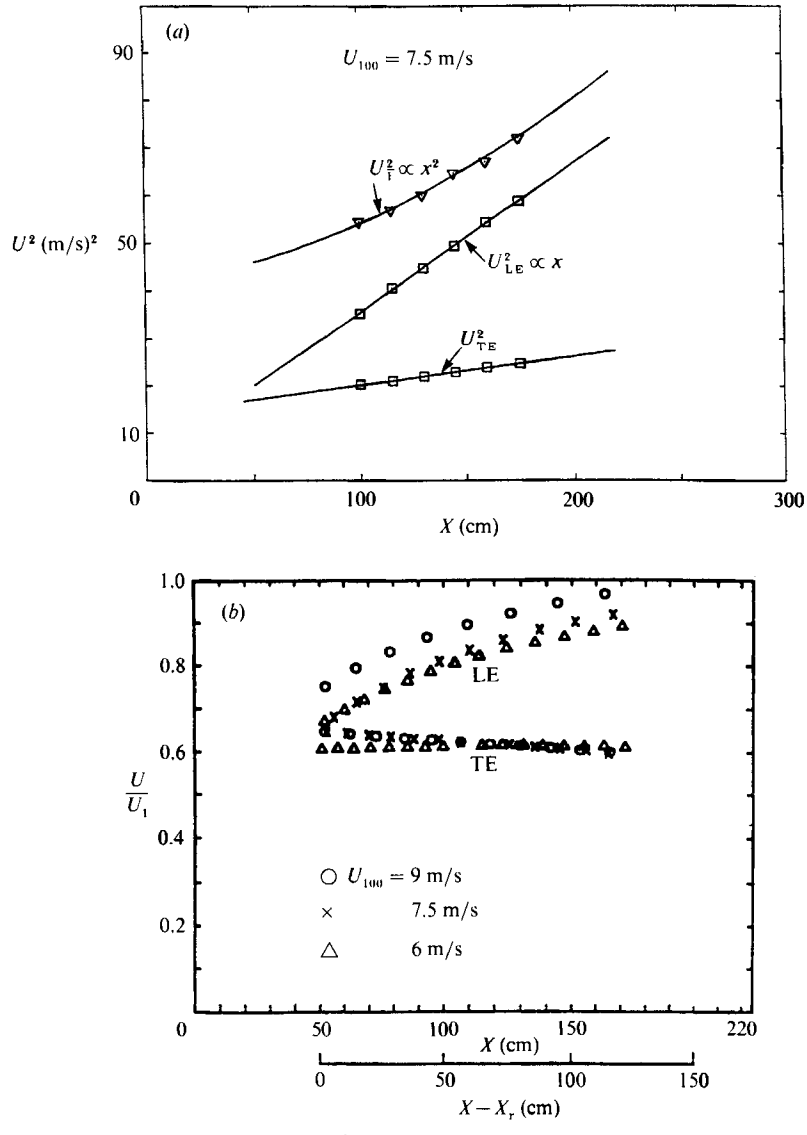


FIGURE 8. The variation of (*a*) $U_1^2$, $U_{LE}^2$ and $U_{TE}^2$ with $X$, and (*b*) $U_{LE}/U_1$ and $U_{TE}/U_1$ with $X$.

symmetry. The laminar velocity profile for each of the three reference velocities considered is plotted on the left-hand side of the figure, and the respective thicknesses of the boundary layers are marked for comparison.

The squares of the celerities calculated for the case cited in figure 4 are plotted in figure 8(*a*) together with the local free-stream velocity measured at six streamwise locations. The celerity of the trailing interface increases slightly with $X$, while the celerity of the leading interface increases with $X$ at a rate that is initially much higher than ($\mathrm{d}U_1/\mathrm{d}X$). Nevertheless, ($U_{LE}/U_1$) is always smaller than unity. The reason for plotting the squares of these celerities in figure 8(*a*) is to demonstrate that both interfaces propagate downstream at a speed that is approximately proportional to $X^{\frac{1}{2}}$ while the free-stream velocity increases linearly with $X$ (figure 3). The procedure was repeated at two additional reference velocities prescribed by $U_{100}$ = 6 and 9 m/s.

The ratio of $U_{TE}/U_1$ plotted in figure 8(*b*) was almost constant at the lowest reference velocity measured (i.e. at $U_{100} = 6$ m/s), while at $U_{100} = 7.5$ and 9 m/s it actually decreases with increasing distance from the leading edge of the plate. The normalized celerities of the leading interface also vary with $X$ and are affected by the choice of $U_r$ (or $U_{100}$). Replotting these celerities as functions of $Re_X = (U_1 X)/\nu$ or $Re_\delta = (U_1 \delta)/\nu$ did not eliminate their dependence on $x$ or on $U_r$. It is clear, therefore, that neither $U_{LE}$ nor $U_{TE}$ scale only with the free-stream velocity outside the boundary layer as they do in the absence of a pressure gradient.

The size and shape of the spot, after its overhang on the plane of symmetry has travelled a distance $(X-X_r)$, can be determined from plots similar to those drawn in figure 5, but in order not to be inundated by data, in view of the large number of independent parameters governing this flow, the results will be presented in a dimensionless form.

### 2.3. *The overall dimensions of the spot*

The state of a boundary layer at some prescribed location can be described by: $U_r$, a reference free-stream velocity; $\delta_r^*$, a characteristic thickness of the laminar boundary layer; $H_r$ a shape factor defining the laminar velocity profile, provided that the fluid is known and the flow is steady, two-dimensional, incompressible and there is no transpiration or heating through the surface. Only $U_r$, however, can be considered as an independent variable while $\delta_r^*$ and $H_r$ depend on $dP/dX$, the pressure gradient which determines the acceleration or deceleration of the free-stream, as well as on $X-X_r$, which defines the streamwise distance from a prescribed reference location.

For the self-similar boundary layer (discussed in §2.1) evolving from a stagnation point located at $X = X_0$, the conditions at the reference location marking the origin of the spot are given by

$$(\delta_r^*)^2 \propto \frac{\nu(X_r - X_0)}{U_{1r}}, \tag{2.11}$$

leading to

$$\frac{X_r - X_0}{\delta_r^*} \propto U_{1r}\frac{\delta_r^*}{\nu} \propto Re_{\delta_r^*}, \tag{2.12}$$

where $\nu$ is the kinematic viscosity of the fluid, while the conditions determining the streamwise evolution of the spot depend on $\beta$ and on $(X-X_r)$ which take into account the pressure gradient and the normalized shape of the velocity profile.

Taking advantage of (2.12), the dimensionless length of the spot on the plane of symmetry may be expressed as a function of three dimensionless parameters and their products:

$$\frac{L_X}{\delta_r^*} = f\left[\beta;\ (Re_{\delta^*})_r;\ \frac{X-X_r}{\delta_r^*}\right]. \tag{2.13}$$

In the absence of a pressure gradient (i.e. for $\beta = 0$), (2.12) still holds except that $U_1 = \text{const.} = U_\infty$ and, consequently, (2.13) becomes

$$\frac{L_X}{\delta_r^*} = f\left[(Re_{\delta^*})_r;\ \frac{X-X_r}{\delta_r^*}\right]. \tag{2.14}$$

Thus for a prescribed $(Re_{\delta^*})_r$, the length of the spot depends only on the distance measured from its origin; experiments indicate that this functional dependence is linear [i.e. $L_X \propto (X-X_r)$] provided $X/X_r$ is large. The dependence of $dL_X/dx$ on the

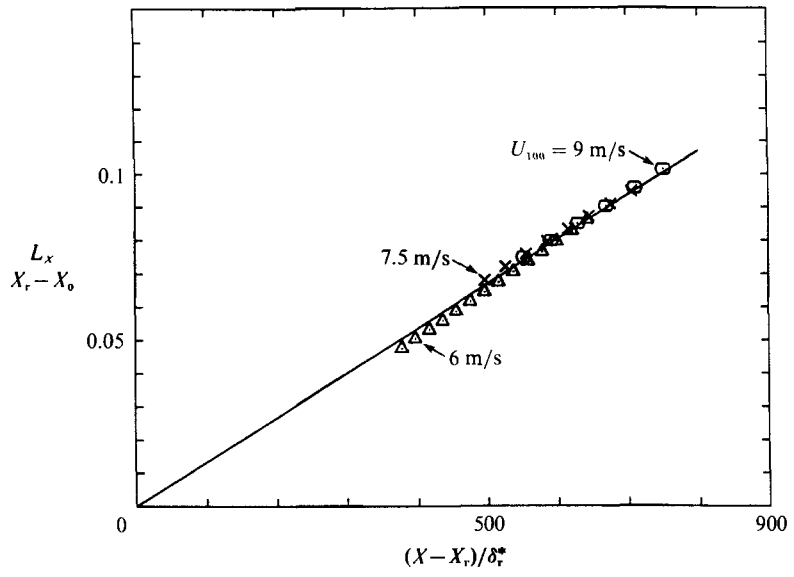


FIGURE 9. The dimensionless length of the spot *vs.* dimensionless distance – the collapse of the data on a single curve.

Reynolds number was given by Wygnanski, Zilberman & Haritonidis (1982) for $600 \leqslant (Re_{\delta^*})_r \leqslant 1520$. For this limited range of Reynolds numbers, a linear fit

$$L_X = [(0.25 + 0.417 \times 10^{-3}\ (Re_{\delta^*})_r]\ (X - X_r) \tag{2.15}$$

represents the data fairly well and is consistent with the dimensional analysis.

Since the virtual origin for the accelerating flow is clearly determined, (2.12) can be used to replace the $\delta_r^*$ appearing on the left-hand side of (2.13) with

$$\frac{X_r - X_0}{(Re_{\delta^*})_r},$$

and since the functional dependence of $L_X$ on $(Re_{\delta^*})_r$ is not defined, (2.13) may be rewritten as

$$\frac{L_X}{X_r - X_0} = f\left[\beta;\ (Re_{\delta^*})_r;\ \frac{X - X_r}{\delta_r^*}\right], \tag{2.16}$$

which for the stagnation flow considered becomes independent of $(Re_{\delta^*})_r$ and may empirically be expressed by

$$\frac{L_X}{X_r - X_0} = 0.134 \times 10^{-3} \left[\frac{X - X_r}{\delta_r^*}\right], \tag{2.17}$$

as shown in figure 9.

The method used to detect the spanwise extent of the spot at $Y \approx 0.6\delta^*$ (i.e. its maximum width) also relies on intermittency, which is difficult to assess when the turbulent signature is weak. We therefore used an array of hot wires which were parallel to the surface and were displaced in the spanwise direction. The total width of the rake containing 12 hot-wire probes was 25 mm and the distance between two adjacent wires was approximately 2 mm. The probe was placed near the anticipated tip of the spot and the velocity recorded by each wire for each event was checked separately. The program singled out two adjacent channels, one of which sensed

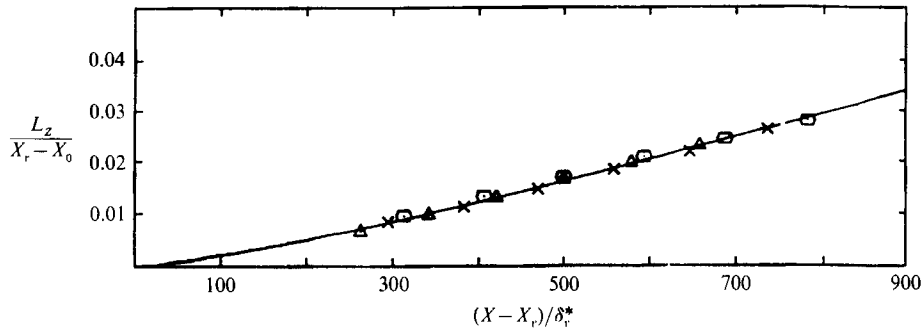


FIGURE 10. the dimensionless span of the spot *vs.* dimensionless $X$.

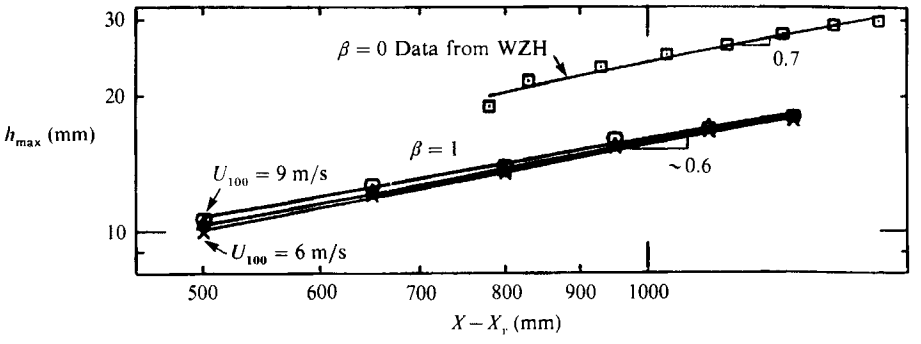


FIGURE 11. The maximum height of the spot *vs.* $X$ (dimensional).

a turbulent signal while the other did not, and the interface was assumed to lie in between. The procedure was repeated for 150 realizations giving the most-probable location tip of the spot at the given $X$-station. The process was repeated at six streamwise locations for the three characteristic velocities considered and the result is presented in figure 10 in the dimensionless form discussed above.

The maximum width of the spot may be approximated by

$$\frac{L_z}{X_r - X_0} = 40 \times 10^{-6}\left[\frac{X - X_r}{\delta_r^*} - 100\right] \tag{2.18}$$

for $(X - X_r)/(\delta_r^*) > 250$, implying that a representative lateral rate of spread of the spot relative to the plane of symmetry is less than 6° rather than the 11° reported in the literature for the flat plate in the absence of a pressure gradient.

The spot spreads in the streamwise and spanwise directions by destabilizing the laminar boundary layer in its vicinity, thus the width and the length of the spot are dependent on the character of the surrounding boundary layer but not its height. The spot is a very flat structure whose typical height is one to two orders of magnitude smaller than its width. Thus, the maximum height of the spot, which is approximately located in the centre of its $(X, Z)$-projection, and is thus totally surrounded by turbulence, cannot be affected by the state of the laminar boundary layer. Since the dimensionless parameters governing the maximum height of the spot are different, the dependence of $h_{max}$ on $(X - X_r)$ is considered in a dimensional form (figure 11).

The maximum height of the spot was determined from local velocity perturbation contours of $-2\%$ rather than from an 'on–off' signal because this procedure was deemed the easiest and most accurate in this case. These contours represent closed

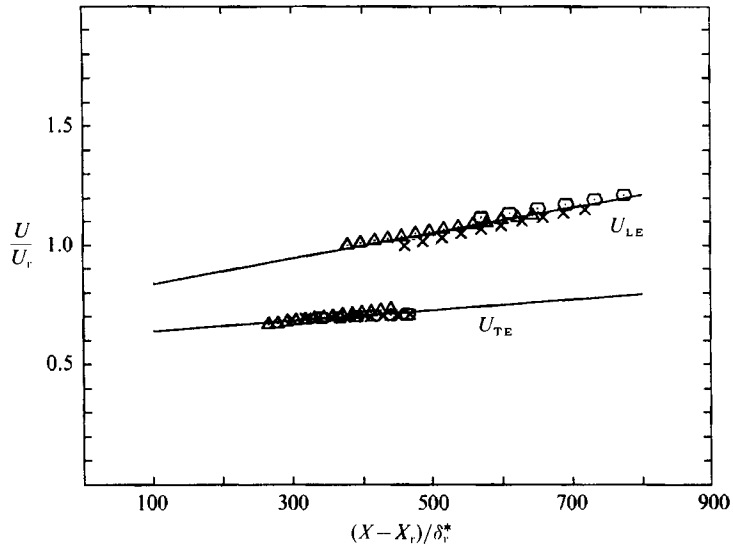


FIGURE 12. The variation of the dimensionless leading- and trailing-edge celerities with dimensionless $X$. The solid curves represent:

$$\left(\frac{U_{LE}}{U_r}\right)^2 = 1.168\times10^{-3}\frac{X-X_r}{\delta_r^*}+0.521, \quad \left(\frac{U_{TE}}{U_r}\right)^2 = 0.306\times10^{-3}\frac{X-X_r}{\delta_r^*}+0.375.$$

loops in which the upper tip of the spot is clearly defined. Although this procedure does not detect turbulence directly, it detects the momentum loss produced by the additional Reynolds stresses and skin friction associated with the passages of turbulence. It is therefore a legitimate, though arbitrary, criterion for the detection of turbulence. This technique was pioneered by Coles & Barker (1975) and was later used by Wygnanski *et al.* (1982) to determine the height of the spot, for which it is most suitable. Although the height of the spot increases with $X$, it is independent of the reference velocity and the surrounding laminar boundary layer. On the other hand, the maximum height of the spot is affected by the size and shape of the surrounding turbulent eddies (i.e. the structure of the surrounding turbulent boundary layer, Schubauer & Klebanoff 1956) and is therefore dependent on the imposed pressure gradient.

In the present investigation (see figure 11), $h_{max} \sim (X-X_r)^{0.6}$ for all three characteristic velocities considered, and compares with $h_{max} \sim (X-X_r)^{0.7}$ determined for $\beta = 0$ by Wygnanski *et al.* (1982). Thus the growth of the spot in the $y$-direction is also reduced by the favourable pressure gradient.

The celerities of the leading and trailing interfaces should also scale with the dimensionless variables outlined in (2.16) such that

$$\frac{U_{int}}{U_r} = f\left[\beta;\ (Re_{\delta^*})_r;\ \frac{X-X_r}{\delta_r^*}\right], \tag{2.19}$$

where $U_{int}$ refers to a celerity of an interface.

The results are plotted in figure 12 for the three reference velocities considered, and once again they seem to be insensitive to $(Re_{\delta^*})_r$. Although the range of $(Re_{\delta^*})_r$ considered here was rather small, a comparable variation in $(Re_{\delta^*})_r$ sufficed to have a significant effect on $U_{TE}$ and $L_X$ in the absence of a pressure gradient (see Wygnanski *et al.* 1982, figure 14).

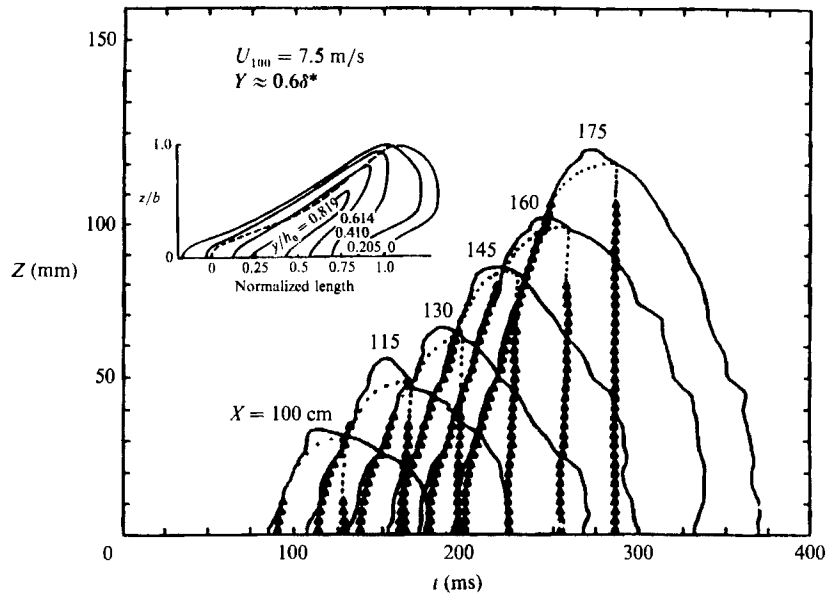


FIGURE 13. The temporal evolution of the spot in the $(t, Z)$-plane compared with a representative shape of the spot in the absence of a pressure gradient.

The temporal evolution of the spot in the $(Z, t)$-plane is shown in figure 13 for $Y/\delta^* = 0.6$ and six streamwise locations. The leading and trailing interfaces determined by intermittency are marked by the triangular symbols. Data points near the tip of the spot were deleted because of the sensitivity of the intermittency signal to threshold level, which might have resulted in an erroneous interpretation. The thick solid lines represent contours of 2% velocity perturbation which coincide with the leading interface of the spot, while the area between the trailing interface and the 2% perturbation contour in the rear of the spot may represent the boundaries of the calmed region.

The difference in shape of the trailing interface between the spot evolving in the Blasius boundary layer and the spot mapped in the present experiment is obvious. For $\beta = 1$ the trailing interface is straight and perpendicular to the plane of symmetry while for $\beta = 0$ the rear turbulent interface of the spot is concave (see insert in figure 13, and also Cantwell *et al.* 1978). The concavity of the turbulent interface is attributed to the breakdown of the wave packet trailing the spot. In the absence of a pressure gradient such a breakdown occurred beyond the critical Reynolds number. This phenomenon was discussed in detail by Glezer *et al.* (1989, e.g. figure 9) for laminar boundary layers evolving at $\beta = 0$ and $\beta = 0.2$. The laminar boundary layer discussed here (i.e. $\beta = 1$), is very stable to small disturbances and therefore the critical $Re$ was never exceeded. Consequently, waves were not anticipated to exist near the tip of the spot over the range of Reynolds numbers considered and the spot was deprived of one of the mechanisms contributing to its growth. The spot may still grow by destabilizing the flow in its vicinity through a strong nonlinear process which probably exists even at subcritical $Re$.

The normalized shape of the spot is approximately self-similar in both $(Y, t)$- and $(Z, t)$-planes, as might be deduced from figure 14, where the boundaries of the spot measured between $100 < (X - X_r) < 175$ collapsed onto a single curve.

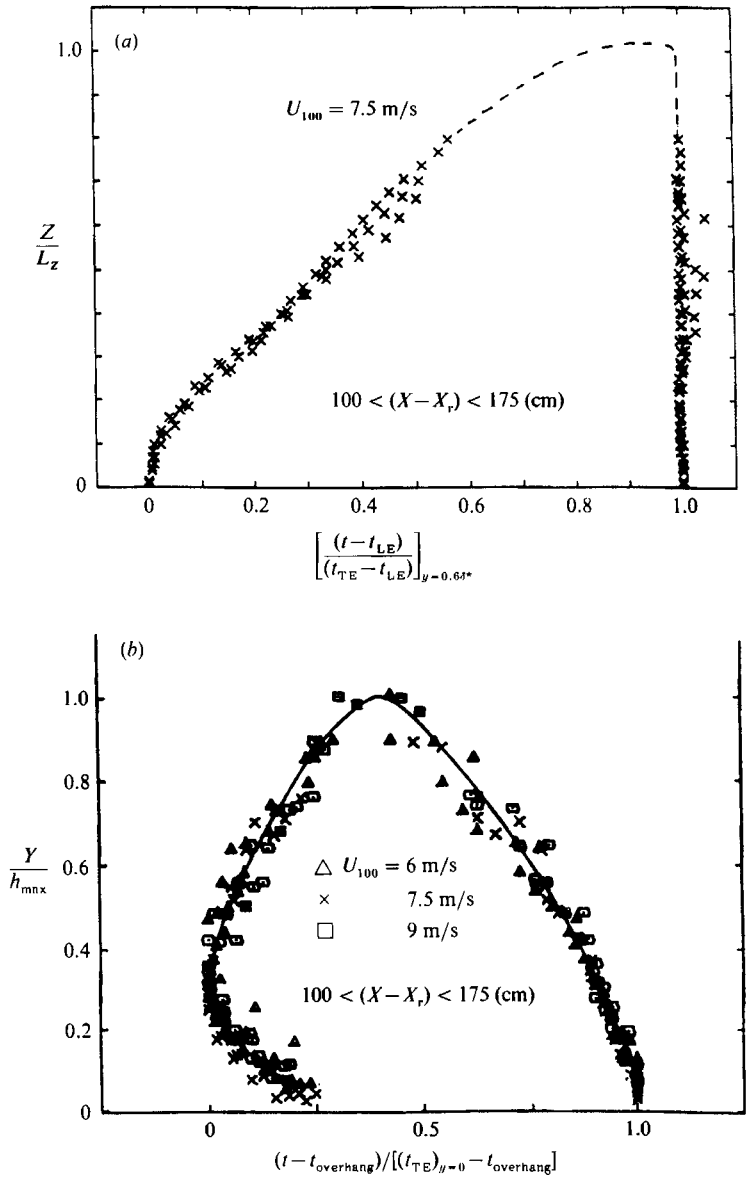


FIGURE 14. Normalized views of the spot: (*a*) plane view, and (*b*) elevation view. $100 < (X-X_r) < 175$ cm.

### 2.4. *The flow field within the turbulent spot and its vicinity*

Some important boundary-layer parameters associated with the passage of the spot far downstream from its origin are plotted in figure 15. These include the displacement thickness $\delta^*$, the momentum thickness $\theta$, and the shape factor $H = \delta^*/\theta$. The variations of these parameters during the passage of the spot in the absence of pressure gradient are known (see Wygnanski *et al.* 1976, p. 808) and can therefore be used to assess the effects of pressure gradient. Both integral lengthscales increase rapidly after the passage of the leading interface and attain their respective maxima at the same time at which the ensemble-averaged boundary of the spot attains its maximum height. They then decrease gradually towards the trailing edge,

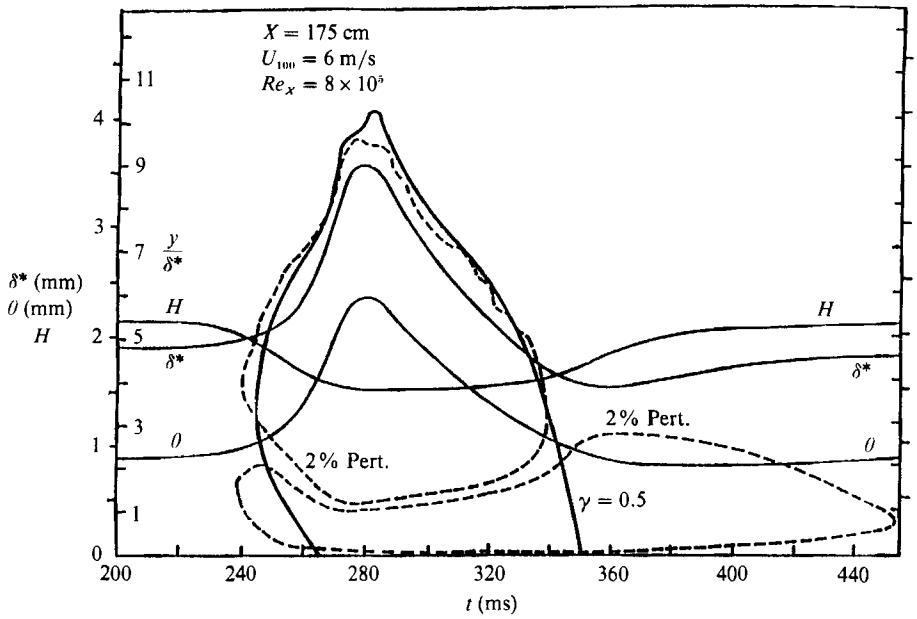


FIGURE 15. The variation of $\delta^*$, $\theta$, and $H$ during the passage of the spot at $Z = 0$.

dipping below their asymptotic values in the undisturbed laminar layer. A qualitatively similar yet quantitatively different behaviour was observed in the absence of pressure gradient.

The thinning of the laminar boundary layer following the spot results in a velocity profile which is more convex and more stable than the ambient profile and was therefore referred to by Schubauer & Klebanoff (1956) as the 'calmed region'. For example, the ratio between the displacement thickness in the calmed region to the displacement thickness computed ahead (downstream) of the leading interface is: $\delta^*_{CR}/\delta^*_{LE} \approx 0.8$ (where the subscript CR refers to the 'calmed region'). In the absence of a pressure gradient, this ratio was as low as 0.57. The momentum thickness behaves in a similar way, but the ratio $\theta_{CR}/\theta_{LE} \approx 0.92$, compared with the ratio of 0.5 in the absence of a pressure gradient. The reduction in the integral scales in both cases (i.e. for $\beta = 1$ and for $\beta = 0$) stems from the change in the shape of the mean velocity profile behind the spot but the overall effect is more significant when the ambient flow is less stable, i.e. it is more notable in the Blasius boundary layer than in the stagnation flow. This may lead one to speculate that the 'calmed region' is generated by the distortion of the local mean flow by some mysterious nonlinear process.

One may also examine the sensitivity of the relative duration of the 'calmed region' to the pressure gradient. This duration may be arbitrarily defined as the time interval between the trailing interface of the spot and the time at which $\delta^*$ returned to within 95% of its undisturbed value or, alternatively, one may replace $\delta^*$ by the shape factor $H$ or use the contour representing a 2% deviation of the ensemble-averaged velocity perturbation as a proper criterion to determine the bounds of the calmed region. Whichever criterion was used, the ratio between the duration of the 'calmed region' and the duration of the turbulent spot, in the present experiment, was approximated unity, i.e. $\Delta T_{CR}/\Delta T_{SP} \approx 1$. The relative duration of the 'calmed region' in the absence of a pressure gradient is approximately 2. Thus, the degree of

instability of the boundary layer surrounding the spot may be linked with the length of the calmed region.

Glezer *et al.* (1989, figure 14) observed that the Tollmien–Schlichting waves following the spot in the absence of a pressure gradient change their spanwise inclination to the flow in the vicinity of the calmed region before 'disappearing' in it. The disappearance of the waves may be more apparent than real because aliasing effects contribute to the apparent elongation of the waves whenever the wave crests are oblique to the plane of measurement. The streamwise streaks observed visually in the calmed region (Gad-el-Hak *et al.* 1981; Cantwell *et al.* 1978) might very well be associated with those waves. Since the visual observations are based on single events they may show the effect more clearly than a somewhat smeared ensemble average of one-dimensional velocity data. One may suggest that in the absence of pressure gradient, the calmed region owes its existence to a nonlinear distortion of the velocity profile by the finite-amplitude waves which turned in the direction of streaming in the wake of the spot. Since the present pressure gradient did not eliminate entirely the calmed region, but only curtailed its dimensions, an additional mechanism might be responsible for the generation of the calmed region. For example it is quite possible that Tollmien–Schlichting waves are embedded in the turbulent region of the spot and they contribute through some nonlinear process to the size of the calmed region.

The shape factor $H$ remains almost constant within the core of the turbulent region, having a value of 1.5 which is typical for a turbulent boundary layer at comparable Reynolds numbers and mildly favourable pressure gradients. The value of $H$ in the unperturbed laminar boundary layer was 2.2, which approximates the theoretical value for a stagnation-point flow. Prior to the arrival of the spot, the value of $H$ decreases from 2.2 to 1.9, indicating that some fluctuations are present in the laminar flow upstream of the spot. This is consistent with linear stability calculations, which identified an unstable region in front of the leading interface of the spot (Glezer *et al.* 1989, figure 17).

A logarithmic velocity distribution (i.e. $U^+ = A\ \log(y^+) + B$) represents the mean flow in the central core of the spot for $10 < y^+ < 200$, where $U^+$ was determined from the slope of the mean velocity profile near the surface. Both $U^+$ and $y^+$ have their customary meaning. The constants $A$ and $B$ varied between 5 and 7, depending on the location of the velocity traverse within the spot, the streamwise distance of the traverse from the origin of the spot, and last but not least an experimental uncertainty in determining the distance between the surface and the hot-wire probe. The results are similar to those recorded in the absence of a pressure gradient (see Wygnanski *et al.* 1976, figure 20) where the logarithmic velocity distribution was observed between $y^+ \approx 20$ and $y^+ \approx 1000$. The extent of the logarithmic velocity distribution in the present experiment was thus significantly shorter than in the absence of a pressure gradient. The 'outer law' or the 'law of the wake' was not observed in either case. In the present experiment, the thickness of the boundary layer did not extent beyond $y^+$ of 200 where $U_1/U^+ \approx 20$.

The turbulent intensity of the streamwise velocity component is a convenient measure by which the transition process and the rate of destabilization of the laminar boundary layer may be gauged. Evaluating the turbulent intensity in a non-stationary flow of the type considered is not trivial; therefore, a special scheme was devised by Glezer *et al.* (1989) in which the data recorded for each realization were processed twice. In the first run, a running average was generated using a variable time window, while in the second run, the turbulent intensity was calculated by

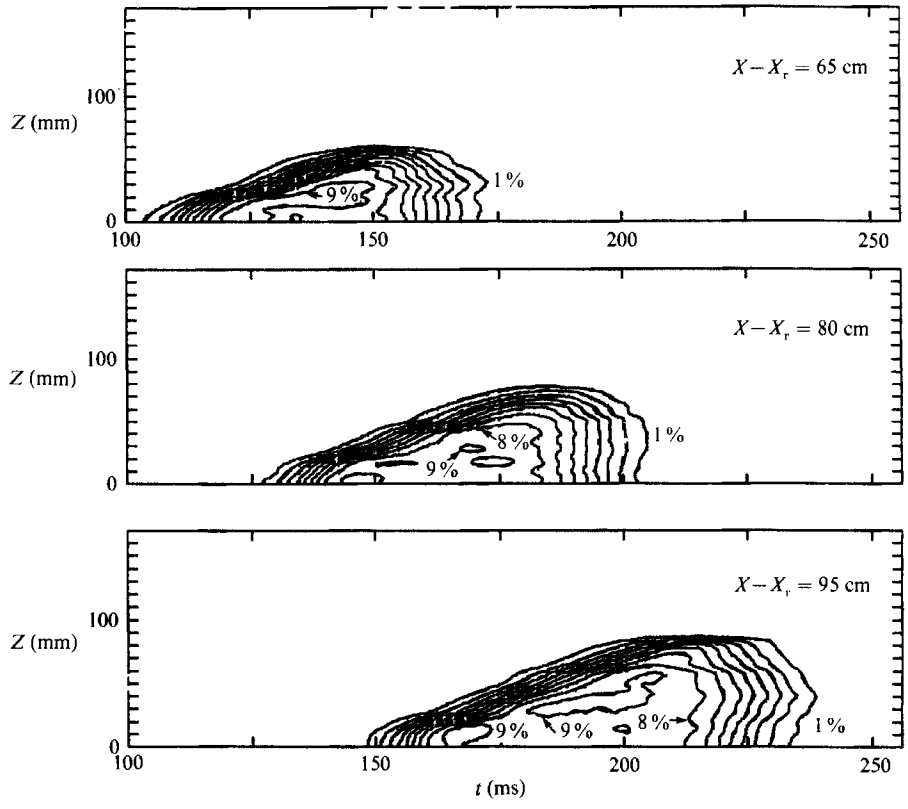


FIGURE 16. Contours of turbulent intensities within the spot at $X-X_r = 65$, 80, and 95 cm and $Y/\delta^* = 0.6$.

subtracting the square of the running average from the square of the recorded time series. The result was dubbed as the 'true r.m.s.'. Since detailed information about the scheme and its validation is provided by Glezer *et al.* (1989), it will simply be used in the present context without further elaboration.

Contours of the dimensionless turbulent intensity ($\langle u'^2\rangle^{\frac{1}{2}}/U_1$) plotted at intervals of 1% in the $(Z,t)$-plane are shown in figure 16 at three different $X$ locations for $U_{100} = 7.5$ m/s. The effect of the pressure gradient may be easily assessed by comparing this figure with figure 6 of Glezer *et al.* (1989). The high turbulent intensity of 9% observed near the tip and the leading interface of the spot at all $X$-locations considered was linked, as before, with the destabilization of the laminar boundary layer. This level of turbulent intensity was observed by Glezer *et al.* (1989) only at the station nearest to the origin of the spot (i.e. at $X_s < 620$ mm). Farther downstream a second turbulent region was detected and the maximum intensity within the original spot *decreased* to 7% and occurred closer to the trailing interface. When the conditions for breakdown of the Tollmien–Schlichting waves trailing the spot do not exist (owing to a low Reynolds number or other stabilizing factors such as a favourable pressure gradient), the secondary source of turbulence generation is cut off and the high-turbulent-intensity region shifted closer to the leading edge of the spot. There were no waves that trailed the spot in the present experiment.

The gradual decrease in the turbulent intensity near the boundaries of the spot stems from averaging the data over spots of different dimensions and shapes; it does not represent a true gradient in the turbulent intensity within the spot. One may also

notice that, in spite of the fact that the turbulent spot evolving in an accelerating flow field is much smaller than its counterpart evolving in the absence of a pressure gradient, the measured turbulent intensities in both are approximately equal provided the Reynolds numbers appropriate to the surrounding laminar boundary layer are subcritical.

## 3. Summary and conclusions

A turbulent spot evolving in a self-similar laminar boundary layer, described by a Falkner–Skan parameter $\beta = 1$, was investigated experimentally. The overall growth of such a spot is significantly inhibited by the favourable pressure gradient, and its spreading rate in both the streamwise and spanwise directions is reduced by more than 50% relative to the corresponding spreading rate of a spot in the absence of a pressure gradient at comparable Reynolds numbers. The favourable pressure gradient used in this experiment did not suffice to squelch the contamination of the laminar flow by turbulence. It helped, however, to reduce the rate of such contamination by eliminating the amplification and breakdown of small-amplitude disturbances because the local Reynolds number was everywhere subcritical.

The propagation rates of the leading and trailing turbulent interfaces no longer scale with the local free-stream velocity as they do in the Blasius boundary layer. While the free-stream velocity increases linearly in the direction of streaming, the propagation of the turbulent interfaces increase as the $X^{\frac{1}{2}}$. The ratio between the propagation velocity of the leading interface to the propagation velocity of the trailing interface increased from approximately 1.2 near the spark location to 1.55 at the last $X$-station at which measurements were taken. The corresponding ratio for the spot evolving in the absence of pressure gradient is approximately 1.8 for the same range of Reynolds numbers.

The trailing interface is nearly straight and perpendicular to the direction of streaming while it often has an arrowhead shape in the absence of a pressure gradient. Since no waves were observed to trail the spot, the generation of secondary turbulent patches resulting from the breakdown of waves was not expected in the range of Reynolds numbers considered (i.e. at $Re_{\delta^*} \approx 10^3$). Above the critical $Re$ for this flow (i.e. at $Re_{\delta^*} > 1.2 \times 10^4$) waves might be generated, changing both the rate of spread of the spot and the shape of its trailing edge. Some linearly unstable regions in the immediate vicinity of the spot, particularly in front of its leading interface might exist even in this pressure gradient. The velocity profile within the spot, as well as some of its integral parameters (such as the displacement thickness, the momentum thickness, and the shape factor), resemble the characteristic parameters of a fully developed turbulent boundary layer. Finally, the turbulent intensity inside the spot is less uniformly distributed but it is somewhat higher than in the corresponding spot evolving in a Blasius boundary layer.

## REFERENCES

CANTWELL, B., COLES, D. & DIMOTAKIS, P. 1978 Structure and entrainment in the plane of symmetry of a turbulent spot. *J. Fluid Mech.* **87**, 641.

CARLSON, D. R., WIDNALL, S. E. & PEETERS, M. F. 1982 A flow visualization of a transition in plane Poiseuille flow. *J. Fluid Mech.* **121**, 487.

CHAMBERS, F. W. & THOMAS, A. S. W. 1983 Turbulent spots, wave packets and growth. *Phys. Fluids* **26**, 1160.

COLES, D. & BARKER, S. J. 1975 Some remarks on synthetic turbulent boundary layers. In *Turbulent Mixing of Reactive and Nonreactive Flows* (ed. S. N. B. Murthy). Plenum.

ELDER, J. W. 1962 An experimental investigation of turbulent spots and breakdown to turbulence. *J. Fluid Mech.* **9**, 235.

EMMONS, H. W. 1951 The laminar turbulent transition in a boundary layer – part I. *J. Aero. Sci.* **18**, 490.

GAD-EL-HAK, M., BLACKWELDER, R. F. & RILEY, J. J. 1981 On the growth of turbulent regions in laminar boundary layers. *J. Fluid Mech.* **110**, 73.

GLEZER, A., KATZ, Y. & WYGNANSKI, I. 1989 On the breakdown of a wave packet trailing the turbulent spot in a laminar boundary layer. *J. Fluid Mech.* **198**, 1.

HENNINGSON, D. S. 1988 The development of localized disturbances in plane Poiseuille flow. Ph.D. thesis, The Royal Institute of Technology, Stockholm.

KACHANOV, Y. S., KOZLOV, V. V. & LEVCHENKO, V. Y. 1979 The development of small amplitude oscillations in laminar boundary-layers. *Fluid Mech. Sov. Res.* **8**, 152.

MORKOVIN, M. V. 1969 On the many faces of transition. In *Viscous Drag Reduction* (ed. C. S. Wells).

NARASIMHA, R. & SABRAMANIAN, C. 1984 Turbulent spot growth in favourable pressure gradients. *AIAA J.* **22**, 837.

ROSS, J. A., BARNES, F. H., BURNS, J. G. & ROSS, M. A. S. 1970 The flat plate boundary layer. Part 3. Comparison of theory with experiment. *J. Fluid Mech.* **43**, 819.

SARIC, W. S. & NAYFEH, A. H. 1975 Nonparallel stability of boundary-layer flows. *Phys. Fluids* **18**, 945.

SCHUBAUER, G. B. & KLEBANOFF, P. S. 1956 Contributions on the mechanics of boundary layer transition. *NACA Rep.* 1289.

SCHUBAUER, G. B. & SKRAMSTAD, H. K. 1948 Laminar boundary layer oscillations on a flat plate. *NACA Rep.* 909.

WAZZAN, A. R., OKAMURA, T. T. & SMITH, A. M. O. 1968 Spatial and temporal stability charts for the Falkner–Skan boundary layer profiles. *McDonnell Douglas Corp. Rep.* DAC 67086.

WYGNANSKI, I. 1981 The effects of Reynolds number and pressure gradients on the transitional spot in a laminar boundary layer. In Lecture Notes in Physics, vol. 136, p. 304.

WYGNANSKI, I., HARITONIDIS, J. & KAPLAN, R. E. 1979 On a Tollmien–Schlichting wave packet produced by a turbulent spot. *J. Fluid Mech.* **92**, 505.

WYGNANSKI, I., SOKOLOV, M. & FRIEDMANN, D. 1976 On a turbulent spot in a laminar boundary layer. *J. Fluid Mech.* **69**, 283.

WYGNANSKI, I., ZILBERMAN, M. & HARITONIDIS, J. 1982 On the spreading of a turbulent spot in the absence of a pressure gradient. *J. Fluid Mech.* **123**, 69.